ABSTRACT

Synthesis of Nitrile TAK-242 Derivatives and Gemfibrozil Analogs

Harold Nguyen

Director: Robert R. Kane, Ph. D

TAK-242 (resatorvid) is a selective antagonist of Toll-like receptor 4 (TLR4) signaling, previously shown to improve transplantation outcomes in a murine model. To further expand the structure-activity relationship of TAK-242, we have synthesized a few analogs of TAK-242. Our approach was to start with a nitrile group in place of the ester to use as a functional handle. These new molecules contain different electron-withdrawing groups on the cyclohexene ring, synthesized from a starting nitrile. This thesis also discusses syntheses of analogs of gemfibrozil, an sGC agonist. To develop a better structure-activity relationship of sGC activators, the aromatic region and carboxylic acid were targeted. The new molecules synthesized are pending biological testing for respective TLR4 inhibition and sGC activation.

APPROVED BY DIRECTOR OF HONORS THESIS:

_____

Dr. Robert R. Kane, Department of Chemistry and Biochemistry

APPROVED BY THE HONORS PROGRAM:

_____

Dr. Elizabeth Corey, Director

DATE: _____

SYNTHESIS OF NITRILE TAK-242 DERIVATIVES AND GEMFIBROZIL ANALOGS

A Thesis Submitted to the Faculty of

Baylor University

In Partial Fulfillment of the Requirements for the

Honors Program

By

Harold Nguyen

Waco, Texas

May 2020

TABLE OF CONTENTS

LIST OF FIGURES

LIST OF SCHEMES

LIST OF ABBREVIATIONS

CD14	Cluster of differentiation 14
cGMP	Cyclic guanosine monophosphate
ESI-HRMS	High resolution electrospray ionization mass spectrometry
gemfibrozil	5-(2,5-dimethylphenoxy)-2,2-dimethyl-pentanoic acid
HMGB1	High mobility group box protein 1
HNOX	Heme Nitric Oxide/Oxygen Domain
HSP	Heat shock protein
IFN-β	Type I interferon Beta
IKK	Inhibitor of nuclear factor kappa B kinase
IL-6	Interleukin 6
IRAK	Interleukin 1 Receptor Associated Kinase
IRF3	Interferon regulatory transcription factor 3
LBP	Lipopolysaccharide binding protein
LPS	Lipopolysaccharide
MAPK	Mitogen-activated protein kinase
MD-2	*also known as* Lymphocyte antigen 96
MyD88	Myeloid differentiation factor 88
NF-κB	Nuclear factor kappa B
NMR	Nuclear magnetic resonance
NO	Nitric oxide

PAH	Pulmonary arterial hypertension
PDE	Phosphodiesterase
RIP1	Receptor-interacting serine/threonine-protein kinase 1
SAR	Structure-activity relationship
sGC	Soluble guanylyl cyclase
TAK1	Transforming growth factor beta-activated kinase 1
TAK-242	Ethyl (6R)-6-[N-(2-chloro-4-fluorophenyl)sulfamoyl]cyclohex-1-ene-1-carboxylate
TIR	Toll/interleukin-1 receptor
TIRAP	Toll/interleukin-1 receptor domain-containing adaptor protein
TLR	Toll-like receptor
TNF	Tumor necrosis factor
TRAF6	Tumor necrosis factor receptor (TNFR)-associated factor 6
TRAM	TRIF-related adaptor molecule
TRIF	TIR-domain-containing adaptor-inducing interferon-β
UBC13	Ubiquitin-conjugating enzyme 13
UEV1A	Ubiquitin-conjugating enzyme E2 variant 1A

ACKNOWLEDGMENTS

I would like to thank Dr. Kane for not only letting me do research in his lab, but also his leadership and guidance in completion of this thesis. I cannot thank Kevin Gayler enough for training and guiding me in my work, and I learned something new every day in lab because of his dedication. I also thank Jeremy, Jessica, and Michael for all their help and kindness, and I thank all the lab members for being supportive and approachable. I thank my committee members for their time and responses. Finally, this work would not have been possible without the support of my family and friends, so I thank my parents, my brother, and real neighbors, skype men, and BQP.

CHAPTER ONE

Introduction to TLR4 and TAK-242

The Toll-like receptor (TLR) family is a series of homologs of the Toll protein in *Drosophila*. In *Drosophila,* Toll plays a role in ontogenesis as well anti-microbial resistance.[1] The TLRs are pattern-recognition receptors expressed by humans and other mammals, as well as other organisms. There are at least 13 known TLRs in mammals, which each detect specific ligands from different sources, such as bacterial cell walls, pathogenic DNA, and autologous products.[2] Thus, the combined, broad range of recognition of pathogenic molecules provided by the TLRs contributes to the immune response in many organisms.

TLR4 is a transmembrane protein which recognizes bacterial lipopolysaccharide (LPS), otherwise known as endotoxin, produced by Gram-negative bacteria. LPS detection leads to release of tumor necrosis factor (TNF) and other pro-inflammatory cytokines, as well as production of Type 1 interferons.[3] Receptor response is initiated by binding of an LPS binding protein (LBP), which carries LPS to TLR4 and transfers it to CD14. CD14 is an anchored protein associated with TLR4 which accepts LPS. LPS is then transferred to MD-2, a protein associated with the extracellular domain of TLR4. TLR4 then homodimerizes by interaction with the intracellular TIR-domains, causing a conformational shift.[4] TLR4 may then act by two pathways, termed MyD88-dependent and MyD88-independent (TRIF-dependent), determined by the adaptor molecules which bind to the new homodimer.[3]

The MyD88-dependent pathway is named after Myeloid differentiation factor 88, a TIR-domain-containing adaptor molecule. In this pathway, TIRAP and MyD88 bind the TIR-domain of TLR4, then recruit death domain-containing molecules IRAK-1 and IRAK-4. TRAF6 then binds to either IRAK and complexes with UBC13 and UEV1A, subsequently activating TAK1. TAK1 activates IKK and MAPK pathways. Downstream of the IKK pathway, NF-κB is translocated, inducing the expression of proinflammatory cytokines and other immune related genes. The MAPK pathway leads to other transcription factor expression, which also helps to activate cytokine expression.[3]

The MyD88-independent (TRIF-dependent) pathway involves TIR domain-containing adaptor inducing IFN-β (TRIF) and TRIF-related adaptor molecule (TRAM). TRIF recruits TRAF3 and RIP1. TRAF3 induces downstream activation of IRF3 which acts with NF-κB to activate transcription of Type-1 interferons.[3] This pathway also induces NF-κB activation through TNF-α production and secretion.[4] The two pathways are shown in Figure 1.1.

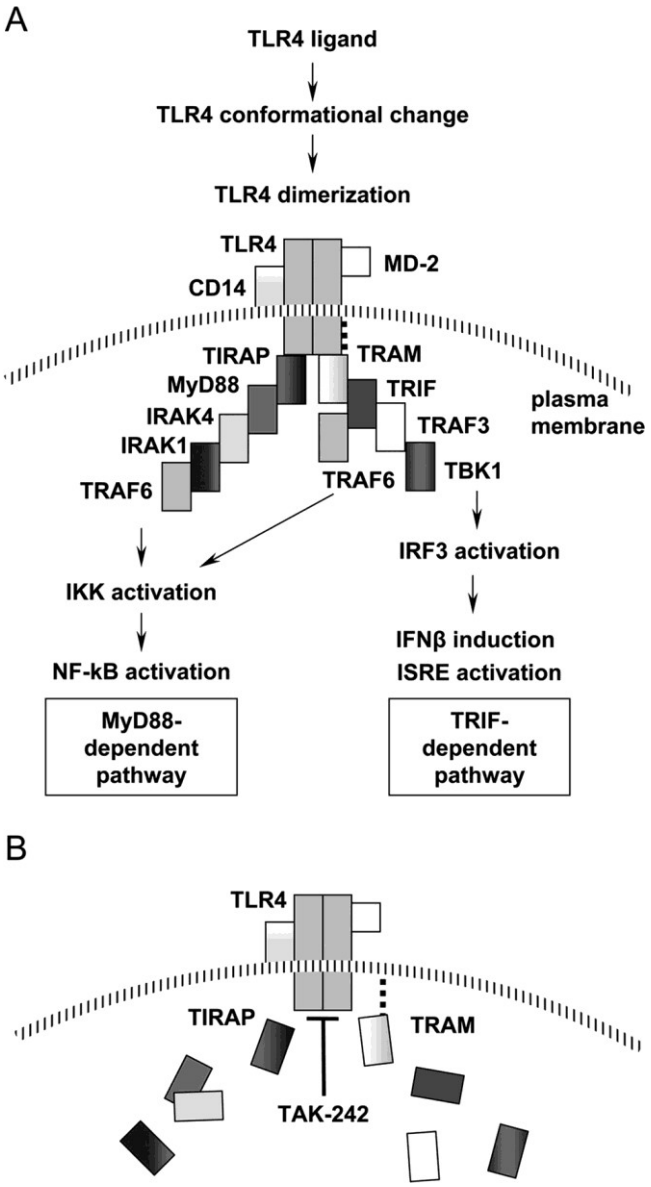

Figure 1.1. (A) Illustration of the TLR4 signaling pathways. (B) Action of TAK-242 disrupts adaptor molecule binding. (Reproduced from reference 12.)

Evidence suggests that TLRs, especially TLR4, are partly responsible for the early innate immune response to transplantation, which can result in graft loss. TLR4 is activated by mediators of inflammation, such as high mobility group box 1 protein (HMGB1), which is released during transplantation. HMGB1 may be passively released

by necrotic cells, or actively released due to cell exposure to TLR agonists.[5] TLR4 likely aids in recognition of HMGB1, as shown by several experiments. The anti-tumor immune response caused by radiation or chemotherapy was shown to be the effect of released HMGB1 from tumor cells acting on TLR4. Mice deficient in HMGB1 or TLR4 lacked the same anti-tumor response.[6] In murine hepatic ischemia-reperfusion models, TLR4 mutant mice lacked an increase in injury after ischemia-reperfusion and exposure to HMGB1, whereas injury increased in the TLR4 wild type.[7] HMGB1 is also released as a result of alloresponse and autoreactivity during transplantation. Other activated immune cells, from acute transplant rejection, can also secrete HMGB1.[5]

Other products released during transplantation include heat shock proteins (HSPs) and hyaluronan. In allograft rejection, HSP production is induced by cell damage, and further transgenic expression has been shown to accelerate rejection.[5] HSP70 binds to several receptors, as well as TLR2 and TLR4, to promote an immune response.[8] Hyaluronan is a polysaccharide found in the extracellular matrix which accumulates during tissue injury, and fragments are suspected to bind to TLR2 and TLR4. Hyaluronan levels have been shown to increase during acute rejection in various rodent allografts, and fragments have been shown to act via a TIRAP-dependent mechanism.[5]

Prevention of the immune response associated with transplantation is normally achieved by systemic administration of immunosuppressants and anti-inflammatories. However, these come with risk of opportunistic infection, nephrotoxicity, and other adverse effects.[9] As TLR4 is implicated in graft rejection, the prevention of tissue damage after transplantation was postulated to be possible by inhibition of TLR4. In pancreatic islets, inhibition of TLR4 using TAK-242 during islet isolation was shown to

lower levels of inflammatory molecules and improve transplantation results in a murine model.[10]

TAK-242 (Ethyl (6R)-6-[N-(2-chloro-4-fluorophenyl)sulfamoyl]cyclohex-1-ene-1-carboxylate, Figure 1.2) is a synthetic drug which inhibits the TLR4 signaling pathway. It is a small molecule developed by Takeda Pharmaceutical Company and was studied in a Phase III clinical trial for the treatment of sepsis.[11] TAK-242 selectively inhibits TLR4 activation. Its mechanism involves disruption of TLR4 and TIRAP or TRAM binding, affecting both MyD88-dependent and MyD88-independent pathways.[12] TAK-242 reacts with Cys747 on the intracellular domain of TLR4 due to its chemical structure containing an α, β-unsaturated carbonyl. Substitution of intracellular Michael donor residues (cysteine to alanine or lysine to arginine) on TLR4 resulted in no change in TAK-242's inhibition of signaling except for alanine substitution of Cys747. Thus, Cys747 is the target of TAK-242. The binding of TAK-242 was shown to not affect TLR4 homodimerization, but it is unclear how TIRAP and TRAM are affected. It was proposed that TAK-242 affects myristoylation or phosphorylation of TIRAP and TRAM, although TAK-242 does not bind to these adaptor molecules.[13]

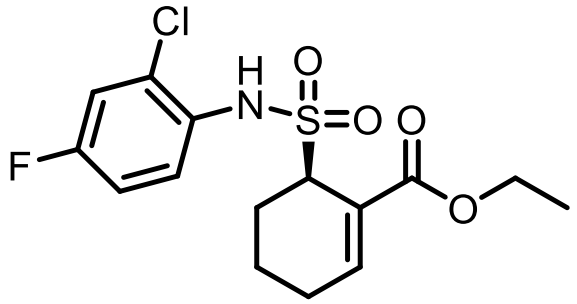

Figure 1.2. Structure of TAK-242.

This report details attempts at synthesizing more effective analogs of TAK-242. TAK-242 is composed of an ethyl ester attached to a cyclohexene base forming a Michael acceptor portion, bridged via a sulfonamide to a phenyl portion. The structure-activity relationship studied by Takeda, based on nitric oxide production inhibition, informed the synthetic background, narrowing our focus to the ethyl ester.[14] The Takeda SAR tested various replacements of the N-arylsulfamoyl portion, switching the halogens and their positions as well as replacing the phenyl ring with other aromatic heterocycles. Halogens increased activity of the molecule. The cyclohexene ring was necessary, as open hexene and benzene replacements had greatly reduced activity. The (S)-enantiomer of TAK-242 showed greatly reduced inhibitory effect on NO, TNF-α, and IL-6 production. The ethyl ester was replaced in a 2,4-difluorophenyl model, showing that an ethyl ester was optimal, although methyl, n-propyl, and isobutyl esters worked almost as well. Isopropyl, n-butyl and hydroxyethyl esters had at least an order of magnitude higher IC_{50}. From these results, it is difficult to ascertain the reason why certain chains are better than others. Mostly pure alkyl chains were tested, and branching patterns do not provide an obvious relationship.

Because the ethyl ester portion is responsible for the Michael acceptor ability, and the SAR results are limited in group diversity at this position, this project was designed to study substitution of this region, with the goal of examining both electronic and steric effects on activity. More effective analogs of TAK-242 could be used in various biological applications, such as transplantation. To be able to access a wider variety of functional groups, including tetrazoles and substituted amides, we synthesized a TAK nitrile intermediate to utilize nitrilium chemistry. Stable N-alkylated nitrilium

intermediates can be made by reaction with Meerwein's salt (Et_3OBF_4) or related compounds. Subsequent hydrolysis could produce secondary amides with different chain lengths, depending on the alkyl chain on the salt. Similarly, addition of an azide to the carbon of a nitrilium species, followed by cyclization, can produce tetrazoles.[15] We looked to use this chemistry to make tetrazole and amide analogs of TAK-242.

CHAPTER TWO

Synthesis of TAK-242 Analogs

The synthetic route that we used to prepare compound **5** is shown in Scheme 2.1, mostly following Takeda's literature procedures.[16,17] Glutaraldehyde was cyclized with a nitrile Horner-Wadsworth-Emmons reagent to afford the base cyclohexene nitrile **2**. This crude product was reacted with acetic anhydride to produce **3.** To produce the aromatic region, a 2-chloro-4-fluoro benzyl thioacetate **5** is synthesized from the benzyl bromide **4** and potassium thioacetate. The thioether **6** was then made from ethanolysis of the thioacetate and addition of **3**. Oxidation of the thioether with m-CPBA then produced the desired sulfone **7**.

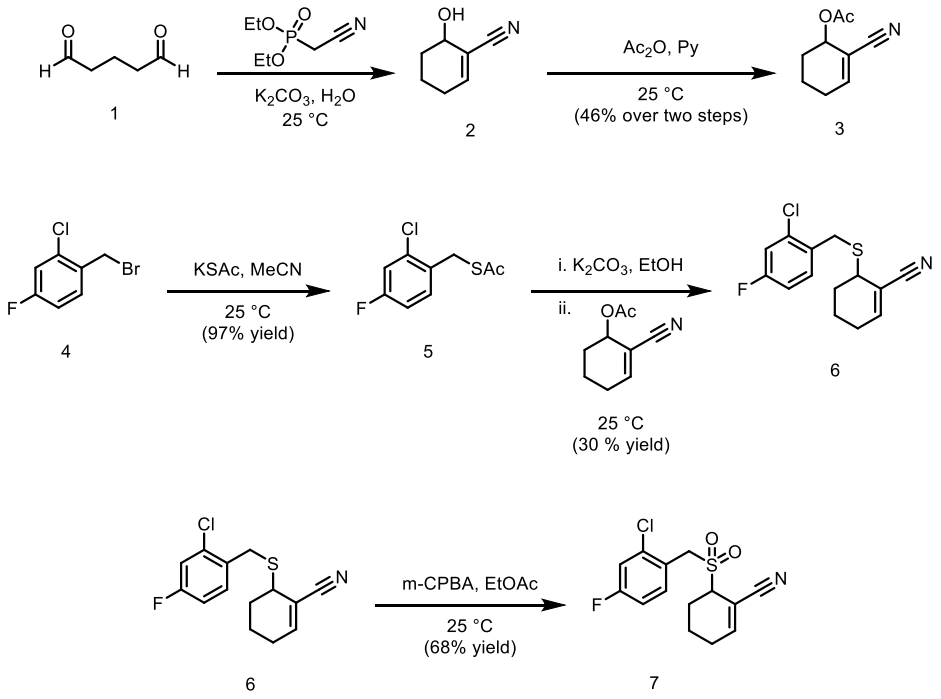

Scheme 2.1. Synthesis of methylene bridge TAK-nitrile.

Besides being another TAK-related compound to test for activity, the nitrile compound was desired for the ability to synthesize a variety of amides using Meerwein salts, which are strong alkylating agents as a result of having three alkyl chains on one oxygen atom. Amide formation follows from a nitrilium intermediate after N-alkylation of the nitrile.[18] A generic mechanism of Meerwein salt alkylation and amide formation is shown in Scheme 2.3. Treatment of **7** with Et_3OBF_4 in DCM, followed by quenching with H_2O in dioxane yielded the ethyl amide TAK product **8** in moderate yield (55%). An analogous reaction with Me_3OBF_4 in DCM, but quenched with distilled water, yielded the corresponding methyl amide **9** in low yield (8%). Further reaction of the ethyl amide with 0.5 M NH_3 in dioxane was unsuccessful in producing the primary amide **10**, and no future attempts were made for producing the primary amide.

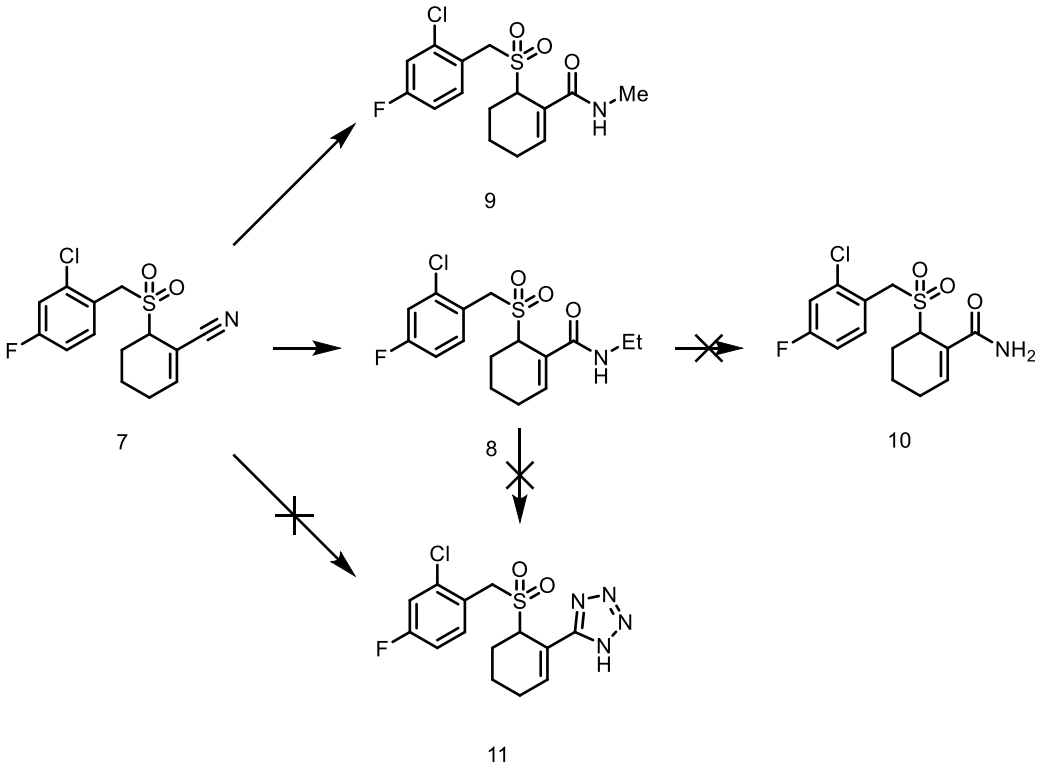

Scheme 2.2. Attempted routes to methylene bridge TAK analogs.

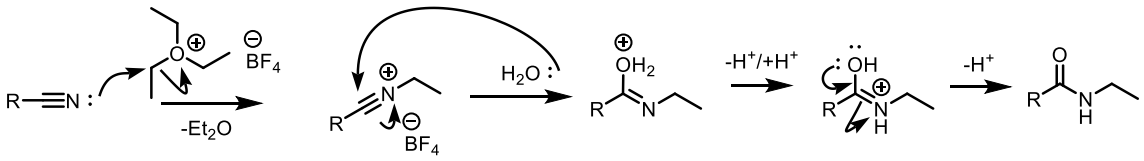

Scheme 2.3. Generic amide formation from a nitrilium intermediate.

The nitrile group also provided a functional handle for tetrazole formation reactions with sodium azide potentially affording **11**. This type of conversion has been demonstrated in a variety of previous tetrazole-containing drug syntheses, and a general mechanism is shown in Scheme 2.4. However, while we made several attempts at the formation of a tetrazole, the product was never isolated. Tetrazoles can typically be prepared by the reaction of nitriles with sodium azide (or other azides) in the presence of a wide range of reagents, such as phosphorous oxychloride, zinc (II) chloride, and ammonium salts. When the TAK nitrile was reacted with phosphorous oxychloride and sodium azide, a tetrazole was thought to have been formed, although attempts at reproducing this result were unsuccessful. The use of sodium azide with TEA·HCL salt in toluene at reflux was suggested in the literature to curb the formation of explosive or reactive byproducts of azide chemistry. However, no tetrazole formation was detected using the salt, so this idea was put aside. Copper catalysts are also often used but were avoided due to possible cell toxicity. The tetrazole literature also suggests the formation of tetrazoles from some amides is possible, though attempts at this were unsuccessful for our molecule. Starting with the ethyl amide TAK, addition of $POCl_3$ and sodium azide in acetonitrile did not provide a discernible product.

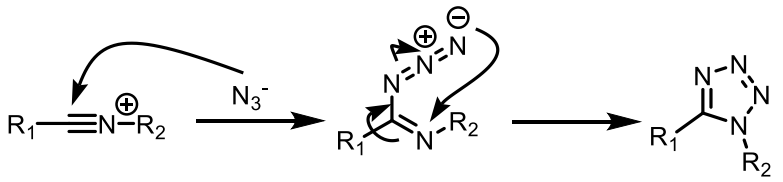

Scheme 2.4. Generic tetrazole formation from a nitrilium intermediate.

Overall, tetrazole derivatives would still be an interesting addition to the SAR of TAK-242 related compounds as tetrazoles can act as bioisosteres of known carboxylic acids. A TAK-242 tetrazole could also potentially be alkylated to give chain lengths similar to the TAK esters known to have activity. The TAK analogs produced will be tested on TLR4 reporter cell assays to determine their inhibitory activity on TLR4 signaling.

Experimental Section

Unless otherwise stated, all reactions were performed in flame-dried glassware under a nitrogen atmosphere, and reagents were used as received. The reactions were monitored by normal phase thin-layer chromatography (TLC) on Millipore glass-backed 60 Å plates (indicator F-254, 250 μM) using the indicated eluents below.

Toluene and Acetonitrile were dried using 4 Å molecular sieves. DCM was dried using KOH and distilled. TEA and DIPEA were distilled from CaH2.

Flash column chromatography was performed using the indicated solvent systems with Silicycle SiliaFlash® P60 (230–400 mesh) silica gel as the stationary phase. 1H and 13C NMR spectra were recorded on either a Bruker Ascend^{TM} 400 spectrometer autosampler or a Bruker Ascend^{TM} 600 autosampler. Chemical shifts (δ) are reported in parts per million (ppm) relative to the residual solvent resonance and coupling constants

(J) are reported in hertz (Hz). NMR peak pattern abbreviations are as follows: s = singlet, d = doublet, dd = doublet of doublets, t = triplet, at = apparent triplet, q = quartet, ABq = AB quartet, m = multiplet. NMR spectra were calibrated relative to their respective residual NMR solvent peaks, CDCl3 = 7.26 ppm (1H NMR)/ 77.16 ppm (13C NMR), DMSO = 2.50 ppm (1H NMR). High resolution mass spectra (HRMS) were obtained in the Baylor University Mass Spectrometry Center on a Thermo Scientific LTQ Orbitrap Discovery spectrometer using +ESI or –ESI and reported for the molecular ion $[M+H]^+$ & $[M+Na]^+$ or $[M-H]^-$ respectively.

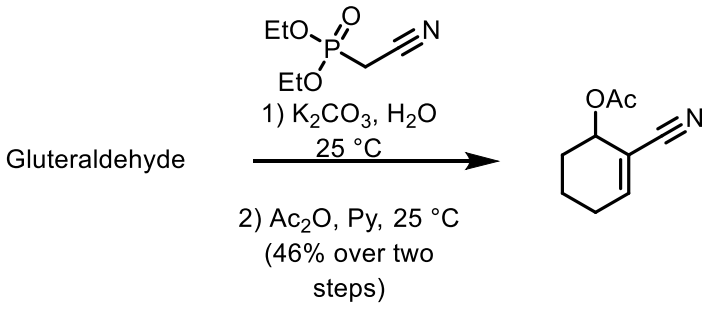

Scheme 2.5. Synthesis of Vinyl Nitrile (3)

The phosphodiester (7.08 g, 40 mmol, 1 equiv.) was added to a solution of 50 wt% glutaraldehyde in H_2O (12 g, 60 mmol, 1.5 equiv.) in a round bottom flask. To the mixture was added K_2CO_3 (12.12 g, 88 mmol, 2.2 equiv.) dissolved in H_2O (26 mL) via addition funnel. Reaction was stirred for 1 h, then extracted with EtOAc. The organic layer was dried with EtOAc and concentrated under vacuum to provide the crude alcohol **2** which was used without further purification.[19]

^{1}H NMR (400 MHz, Chloroform-*d*) δ 6.75 (t, *J* = 4.0, 1.0 Hz, 1H), 4.34 – 4.26 (m, 1H), 2.32 – 2.22 (m, 1H), 2.21 – 2.10 (m, 1H), 1.96 – 1.86 (m, 1H), 1.85 – 1.72 (m, 2H), 1.69 – 1.56 (m, 1H).

The crude alcohol was dissolved in Ac_2O (20 mL), followed by addition of pyridine (16.5 mL). Reaction was stirred for 20 hr, then extracted with EtOAc and washed with 1 M HCl. The reaction mixture was purified by column chromatography using a 30:70 EtOAc:Hex gradient providing 2.81 g of a colorless oil in 46% yield over two steps.[20]

^{1}H NMR (400 MHz, Chloroform-*d*) δ 6.87 (t, *J* = 4.0, 1.0 Hz, 1H), 5.41 (t, *J* = 6.7, 3.5, 1.3 Hz, 1H), 2.38 – 2.26 (m, 1H), 2.26 – 2.14 (m, 1H), 2.12 (s, 3H), 1.98 – 1.84 (m, 2H), 1.85 – 1.67 (m, 2H).

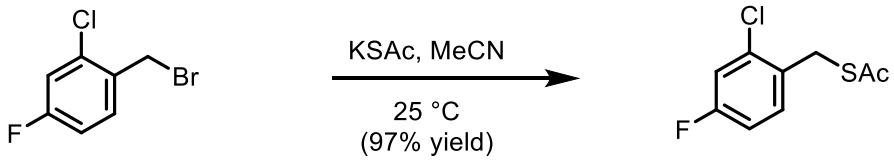

Scheme 2.6. Synthesis of Benzylic Thioacetate (5)

The benzylic bromide (2.00 g, 8.9 mmol, 1 equiv.) was added to a 6-dram vial, followed by KSAc (1.12 g, 9.79 mmol, 1.1 equiv.) and MeCN (8 mL). Reaction was stirred for 4 h at 25 °C. Reaction was diluted with EtOAc, filtered, then washed with H_2O. The organic layer was separated, dried with sodium sulfate, and concentrated under vacuum to provide 1.88 g of a yellow oil in 97% yield.[17]

^{1}H NMR (600 MHz, Chloroform-*d*) δ 7.42 (dd, *J* = 8.6, 6.0 Hz, 1H), 7.10 (dd, *J* = 8.5, 2.6 Hz, 1H), 6.91 (td, *J* = 8.3, 2.6 Hz, 1H), 4.17 (s, 2H), 2.33 (s, 3H).

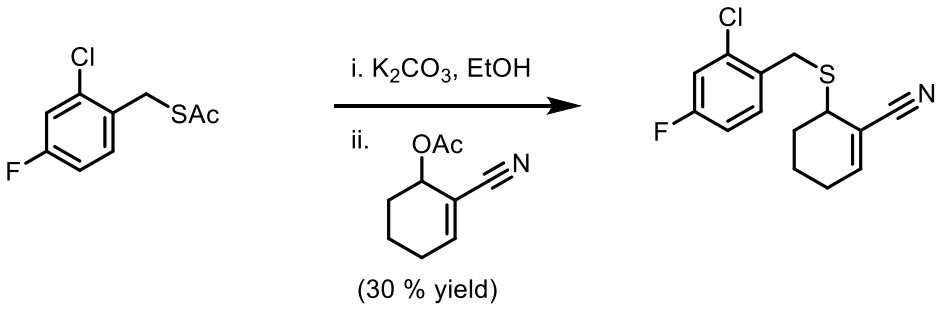

Scheme 2.7. Synthesis of Thioether (6)

K_2CO_3 (1.6 g, 11.5 mmol, 2.3 equiv.), the thioacetate (1.0 g, 4.6 mmol, 1 equiv.), and EtOH (4.6 mL) were added to a 6-dram vial and stirred at 25 °C for 15 h, when the allylic acetate (760.0 mg, 4.6 mmol, 1 equiv.) was added and stirred at 25 °C for 5 h. Reaction was concentrated, then diluted with EtOAc and washed with H_2O. The organic layer was separated and dried with sodium sulfate. Reaction mixture was purified by column chromatography using a 10:90 to 20:80 EtOAc:Hex gradient to provide 392 mg of a white solid in 30% yield.

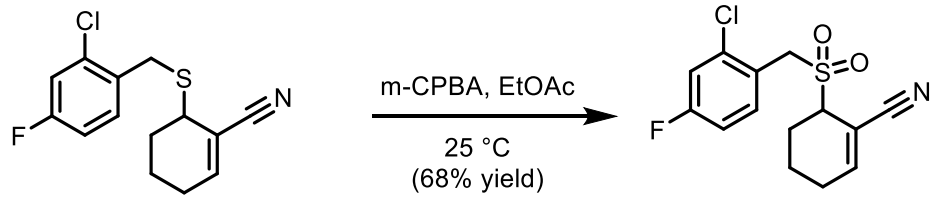

Scheme 2.8. Synthesis of Sulfone (7)

The thioether (382.2 mg, 1.36 mmol, 1 equiv.), 77 wt% mCPBA (670.3 mg, 2.99 mmol, 2.2 equiv.), and EtOAc (13 mL) were added to a 6-dram vial. Reaction was stirred for 1.5 h at 25 °C, then washed with sat. Na_2CO_3. The organic layer was separated and

dried with sodium sulfate. Reaction mixture was purified by column chromatography 20:80 then 50:50 EtOAc:Hex to provide 291.0 mg of a white solid in 68% yield.

^{1}H NMR (400 MHz, Chloroform-*d*) δ 7.60 (dd, *J* = 8.7, 5.9 Hz, 1H), 7.23 (dd, *J* = 8.4, 2.6 Hz, 1H), 7.15 (t, *J* = 4.1 Hz, 1H), 7.10 – 7.03 (m, 1H), 4.70 (d, *J* = 13.9 Hz, 1H), 4.59 (d, *J* = 13.9 Hz, 1H), 3.84 – 3.80 (m, 1H), 2.56 – 2.39 (m, 2H), 2.35 – 2.23 (m, 1H), 2.13 – 2.00 (m, 1H), 1.91 – 1.81 (m, 1H), 1.81 – 1.72 (m, 1H).

^{13}C NMR (151 MHz, Chloroform-*d*) δ 162.9 (d, *J* = 253.2 Hz), 154.2, 136.3, 134.4, 121.3, 118.2, 117.6 (d, *J* = 25.1 Hz), 115.0 (d, *J* = 21.4 Hz), 105.7, 58.2, 56.0, 25.7, 21.8, 16.9.

+ESI-HRMS m/z: calc'd for $C_{14}H_{13}ClFNNaO_2S$ $[M+Na]^+$ = 336.0237, found $C_{14}H_{13}ClFNNaO_2S$ = 336.0234.

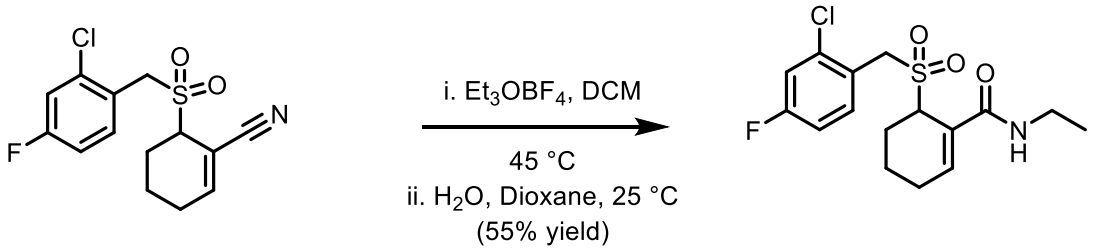

Scheme 2.9. Synthesis of Ethyl Amide (8)

The nitrile (100.0 mg, 0.32 mmol, 1 equiv.) and DCM (0.6 mL) were added to a vial, followed by Et_3OBF_4 (121.1 mg, 0.64 mmol, 2 equiv.) and sealed and heated to 45 °C for 24 h. Half of the reaction mixture was transferred to a vial containing 1 mL of a 1:10 H_2O:Dioxane mixture and stirred for 22 h, then diluted with EtOAc and washed with brine. The organic layer was separated and dried with sodium sulfate. Reaction was purified by column chromatography using a 20:80 to 40:60 to 50:50 to 60:40 EtOAc:Hex

gradient. Further purification of the product-containing fractions was done via column chromatography using 40:60 Acetone:Hex to provide 32.0 mg of a white solid in 55% yield based on the half of the solution used for this condition.

^{1}H NMR (400 MHz, Chloroform-*d*) δ 7.59 (dd, *J* = 8.7, 6.0 Hz, 1H), 7.19 (dd, *J* = 8.5, 2.7 Hz, 1H), 7.02 (td, *J* = 8.2, 2.7 Hz, 1H), 6.71 (t, *J* = 3.9 Hz, 1H), 6.01 (s, 1H), 4.62 – 4.56 (m, 1H), 4.52 (d, *J* = 13.7 Hz, 1H), 4.46 (d, *J* = 13.8 Hz, 1H), 3.43 – 3.34 (m, 2H), 2.50 (dt, *J* = 14.5, 2.9 Hz, 1H), 2.42 – 2.30 (m, 1H), 2.25 – 2.13 (m, 1H), 2.05 – 1.91 (m, 1H), 1.79 – 1.64 (m, 2H), 1.20 (t, *J* = 7.3 Hz, 3H).

^{13}C NMR (151 MHz, Chloroform-*d*) δ 168.2, 162.7 (d, *J* = 252.0 Hz), 138.4, 136.5 (d, *J* = 10.5 Hz), 134.1 (d, *J* = 9.2 Hz), 128.9, 122.1 (d, *J* = 3.9 Hz), 117.5 (d, *J* = 24.9 Hz), 114.6 (d, *J* = 21.5 Hz), 56.9, 56.5, 34.9, 24.8, 22.5, 17.6, 14.7.

+ESI-HRMS m/z: calc'd for $C_{16}H_{19}ClFNNaO_3S^+$ $[M+Na]^+$ = 382.0650, found $C_{16}H_{19}ClFNNaO_3S^+$ = 382.0657.

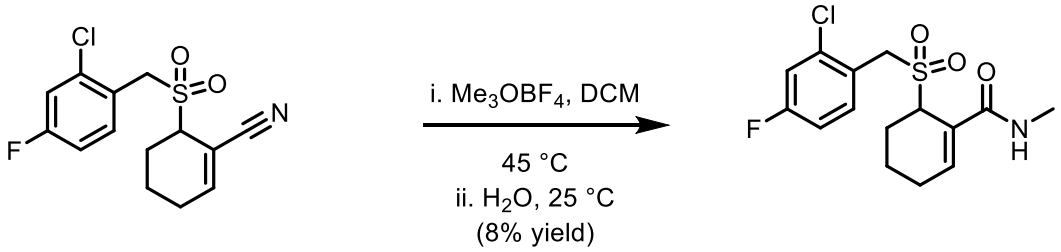

Scheme 2.10. Synthesis of Methyl Amide (9)

The nitrile (100.0 mg, 0.32 mmol, 1 equiv.), DCM (0.9 mL), and Me_3OBF_4 (188.5 mg, 1.27 mmol, 4 equiv.) were added to a sealed 1-dram vial and stirred at 45 °C for 53 h, then quenched with water and extracted with DCM. The organic layer was dried with

sodium sulfate, then filtered. The crude mixture was purified with column chromatography using a 20:80 to 40:60 to 50:50 EtOAc:Hex gradient to provide 9.1 mg of a white solid in 8% yield.

^{1}H NMR (600 MHz, Chloroform-*d*) δ 7.60 (dd, *J* = 8.6, 6.0 Hz, 1H), 7.20 (dd, *J* = 8.4, 2.6 Hz, 1H), 7.05 – 7.01 (m, 1H), 6.03 (d, *J* = 5.4 Hz, 1H), 4.60 (d, *J* = 5.7 Hz, 1H), 4.55 – 4.46 (m, 2H), 2.91 (d, *J* = 4.9 Hz, 3H), 2.53 – 2.46 (m, 2H), 2.35 (ddd, *J* = 19.9, 7.8, 3.5 Hz, 1H), 2.24 – 2.15 (m, 1H), 2.01 – 1.91 (m, 1H), 1.78 – 1.65 (m, 2H).

^{13}C NMR (151 MHz, Chloroform-*d*) δ 169.1, 162.9 (d, *J* = 252.4 Hz), 138.6, 134.2 (d, *J* = 9.0 Hz), 128.9, 122.3, 117.6 (d, *J* = 24.9 Hz), 114.8 (d, *J* = 21.4 Hz), 57.1, 56.6, 26.9, 24.9, 22.7, 17.7.

+ESI-HRMS m/z: calc'd for $C_{15}H17ClFNNaO_3S$ $[M+Na]^+$ = 368.0499, found 368.0492.

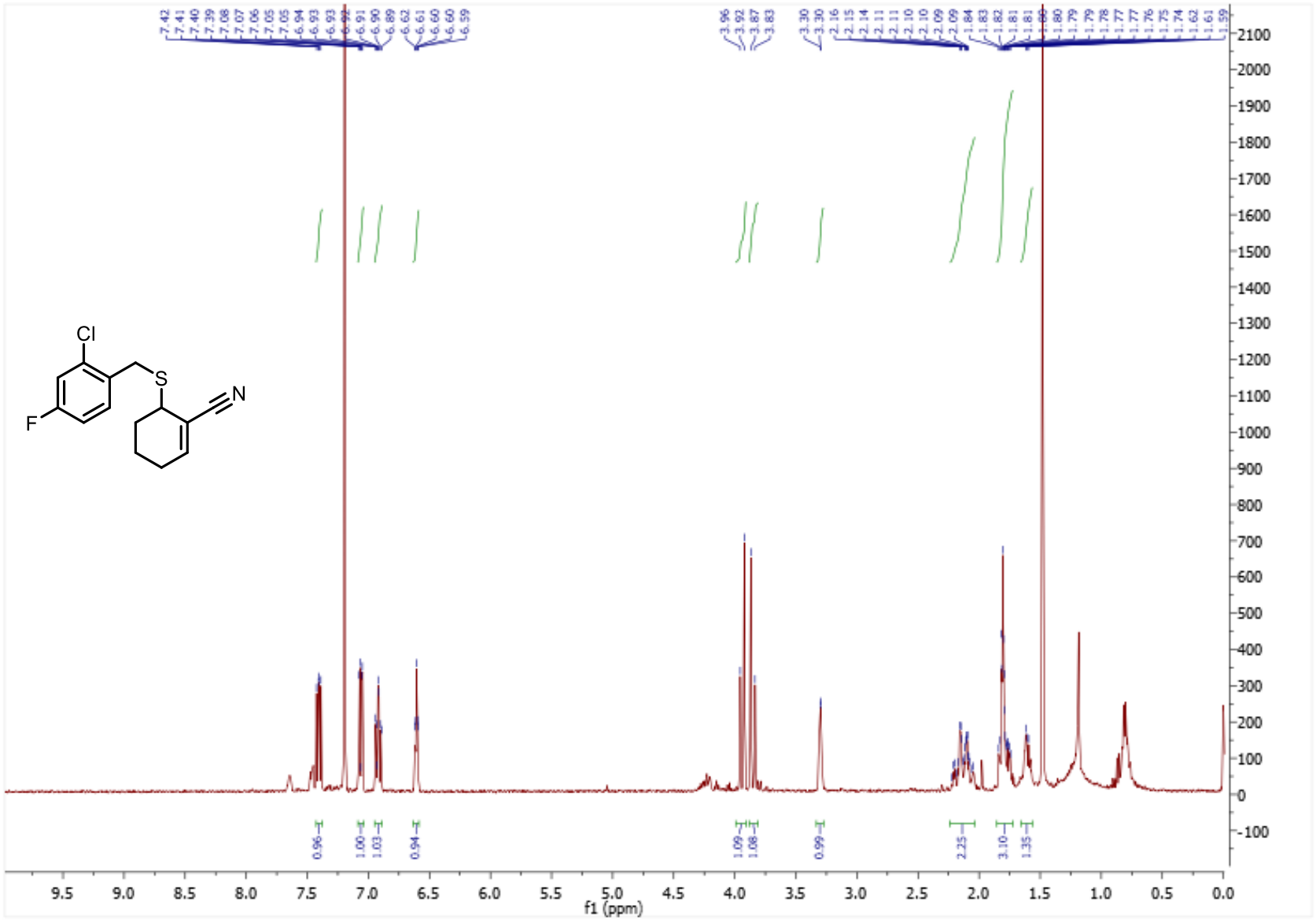

Figure 2.1. ^{1}H NMR of Thioether (6).

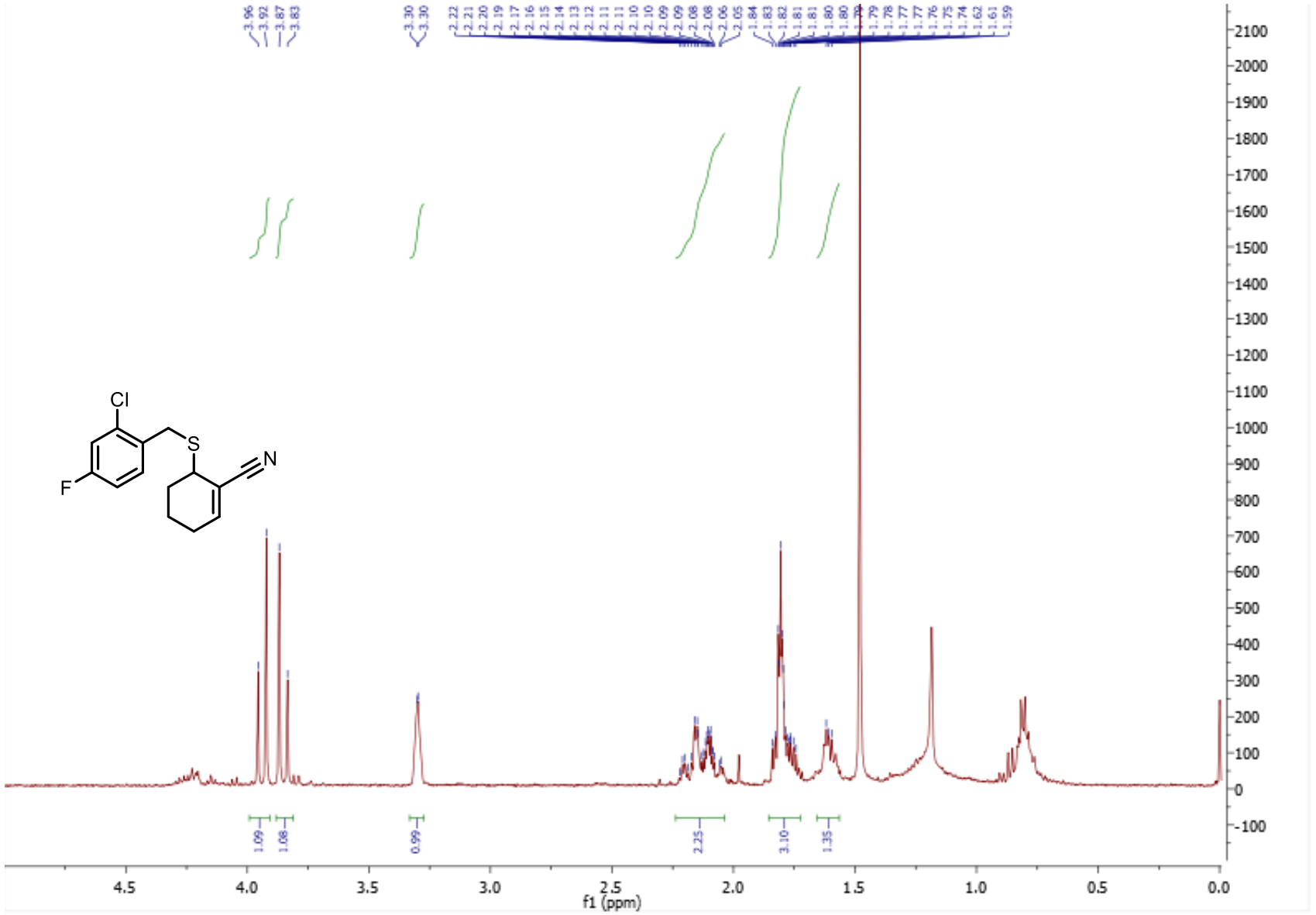

Figure 2.2. ^{1}H NMR of Thioether (6) (0-5 ppm inset).

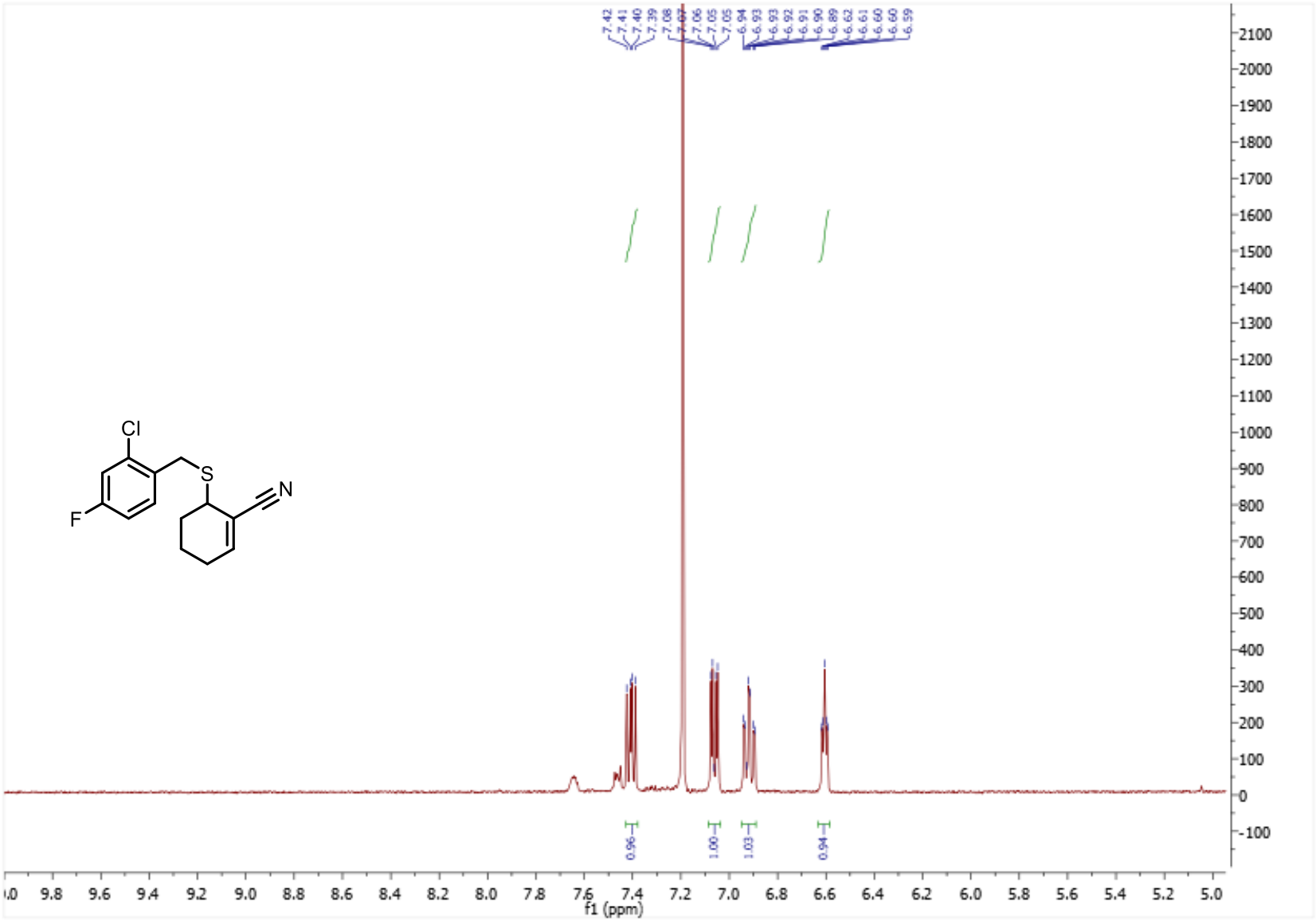

Figure 2.3. ^{1}H NMR of Thioether (6) (5-10 ppm inset).

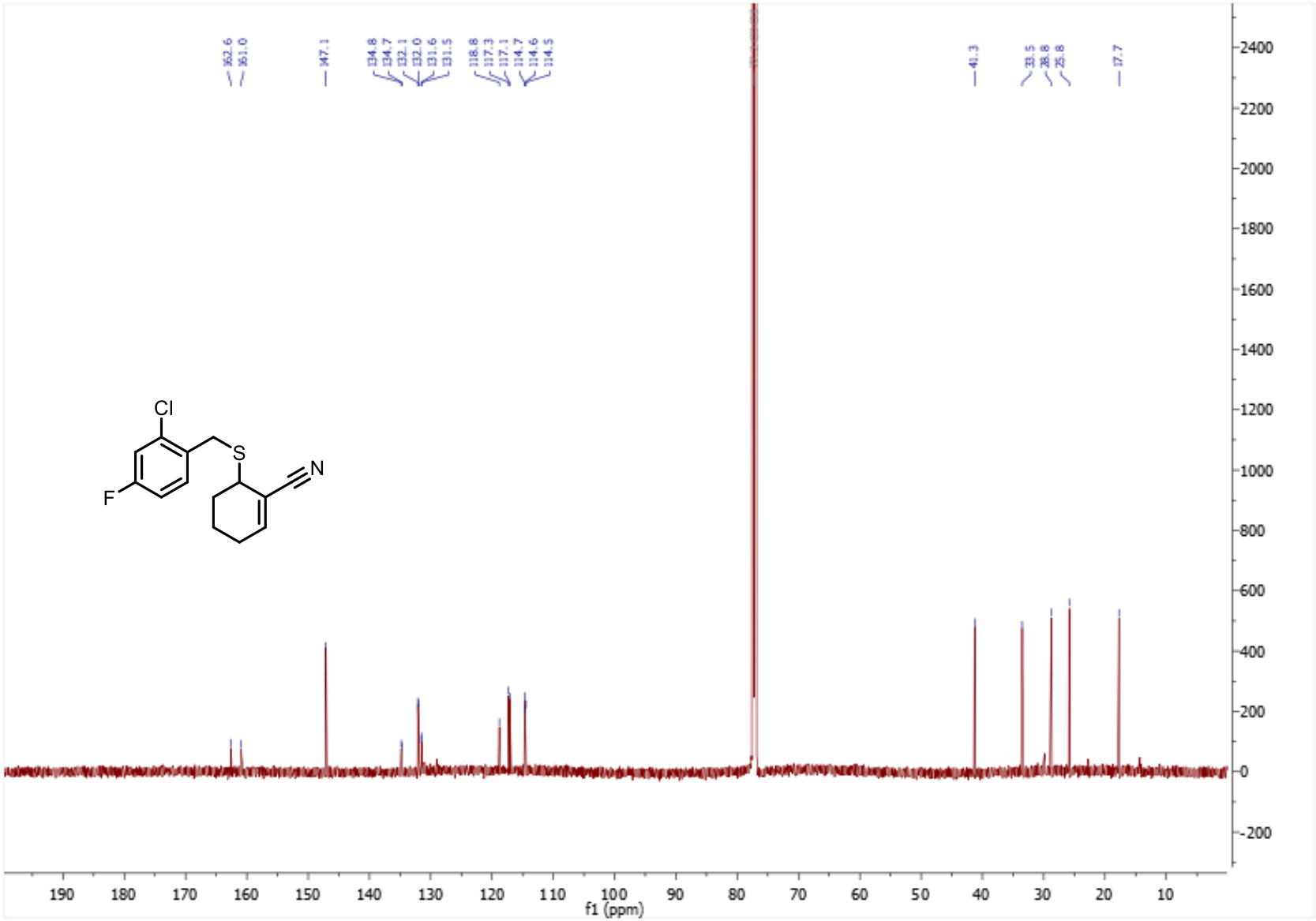

Figure 2.4. ^{13}C NMR of Thioether (6).

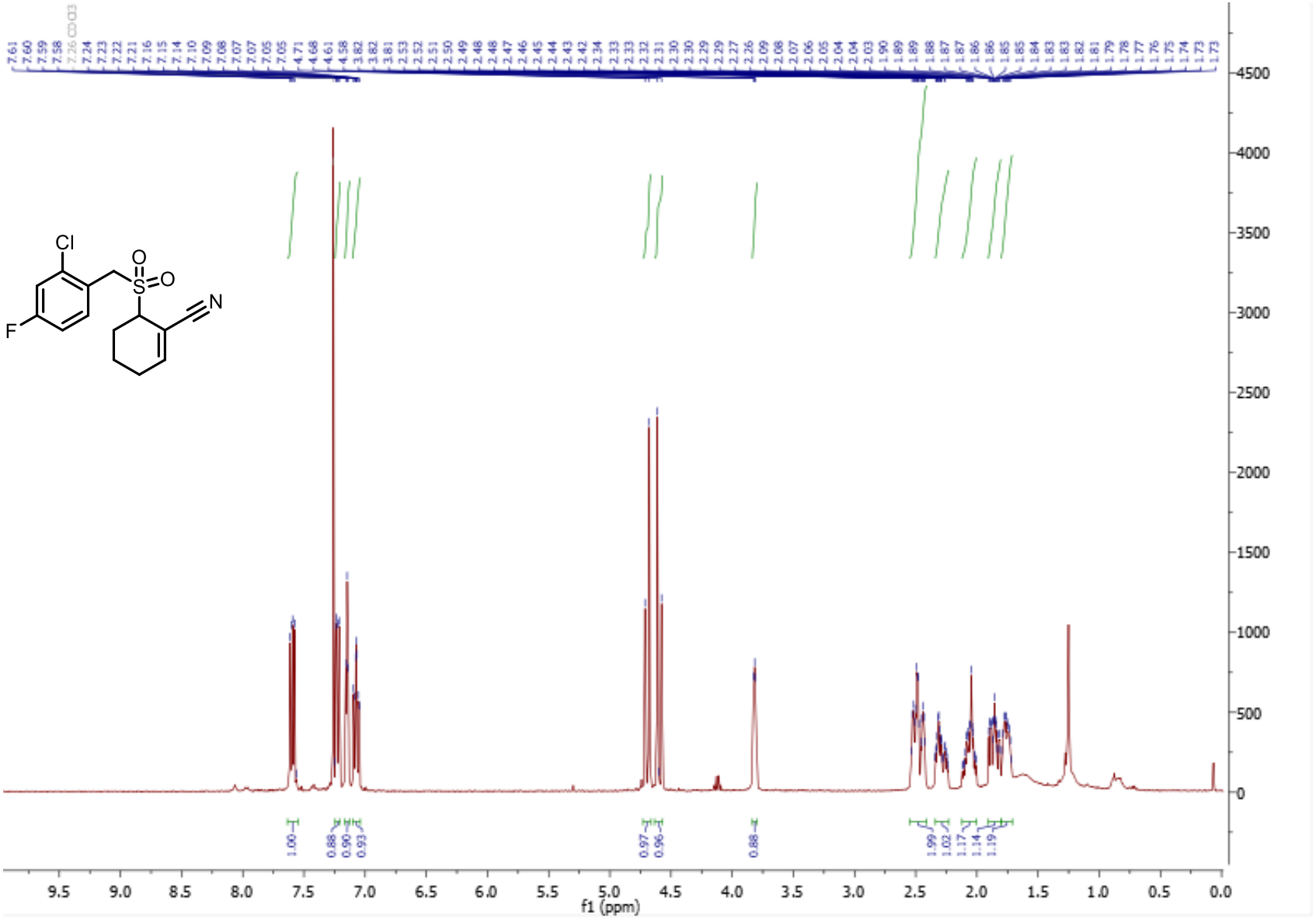

Figure 2.5. ^{1}H NMR of Sulfone (7).

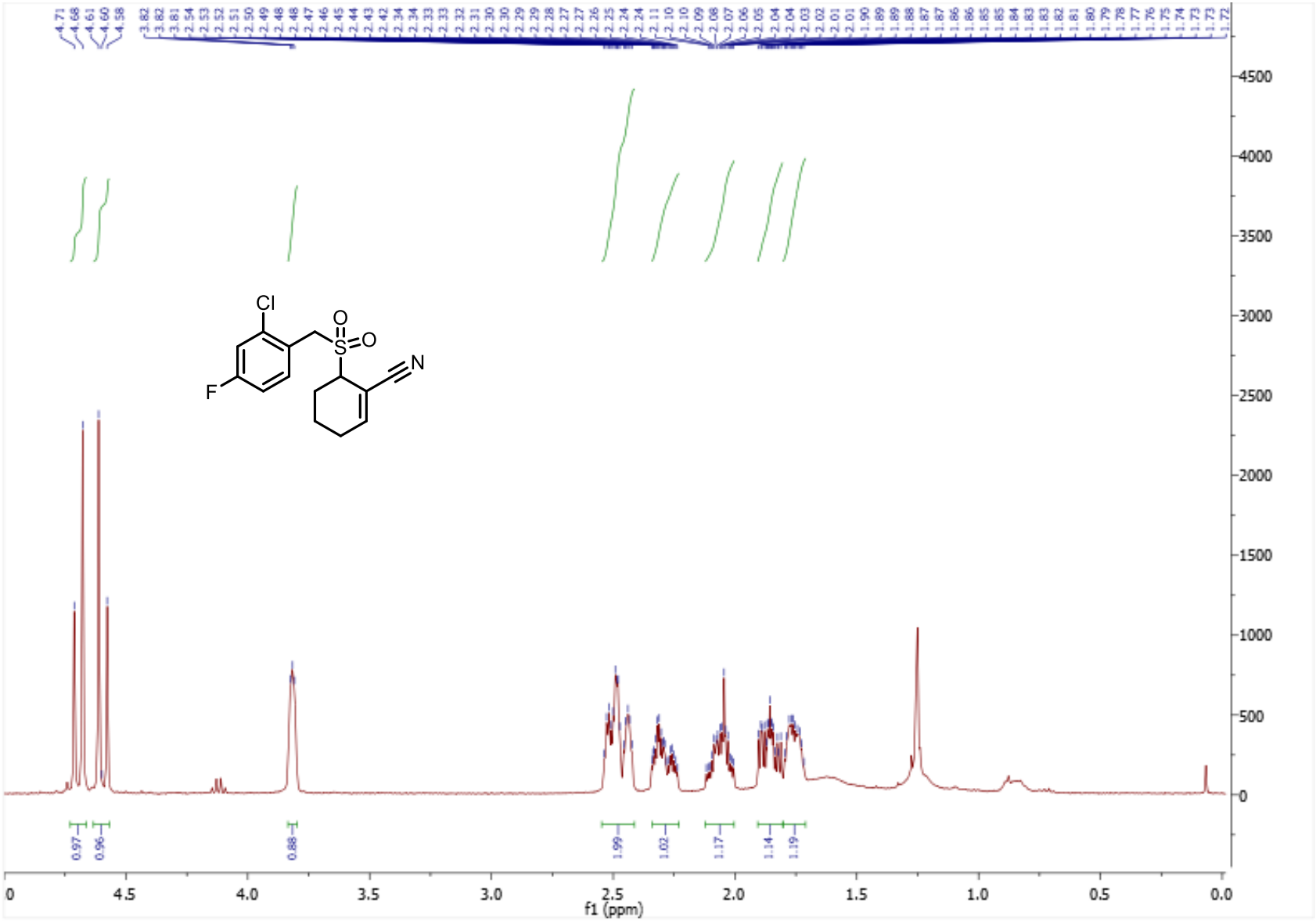

Figure 2.6. ^{1}H NMR of Sulfone (7) (0-5 ppm inset).

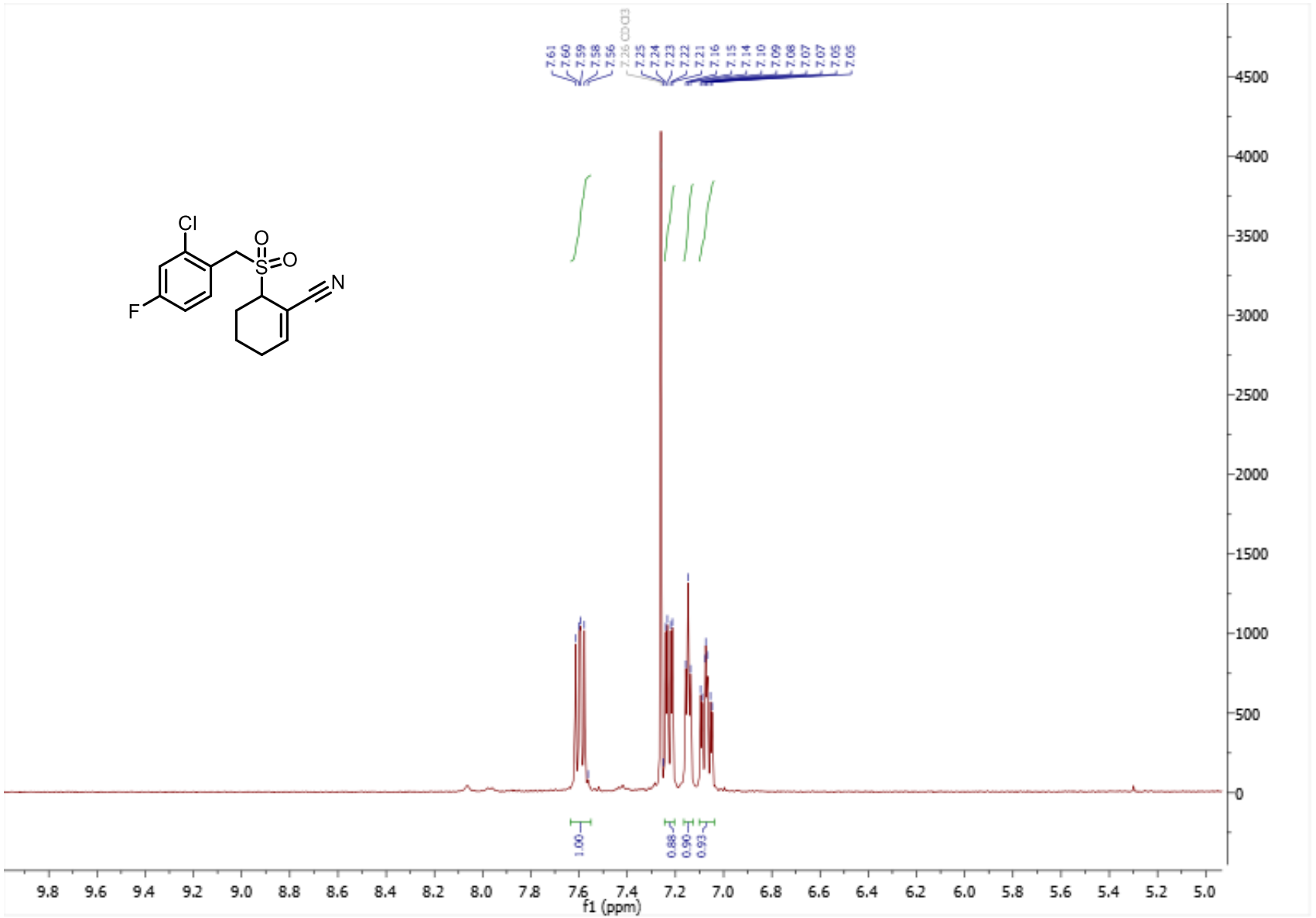

Figure 2.7. ^{1}H NMR of Sulfone (7) (5-10 ppm inset).

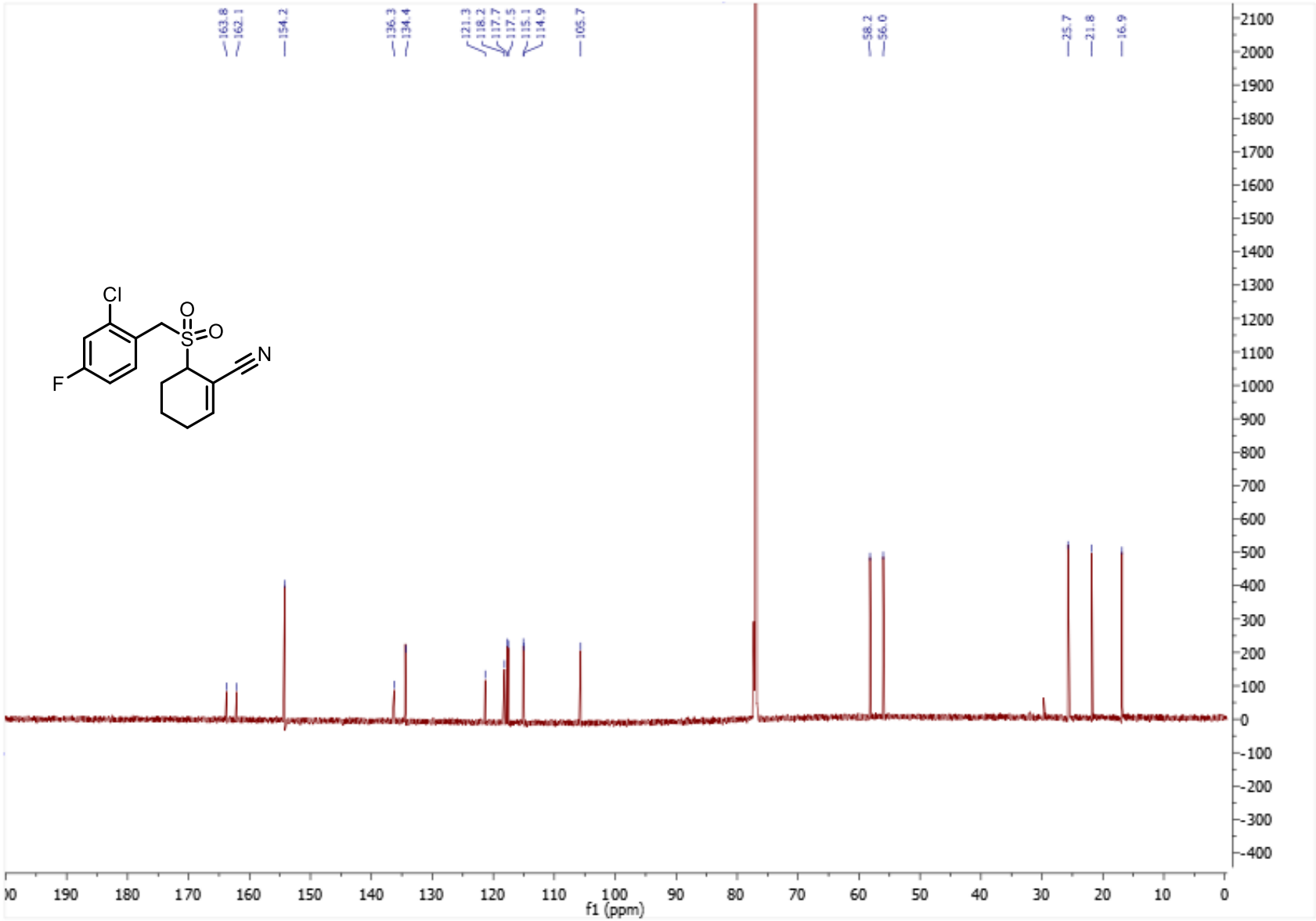

Figure 2.8. ^{13}C NMR of Sulfone (7).

CHAPTER THREE

Introduction to sGC and Gemfibrozil

Nitric oxide (NO) signaling is a unique pathway in animals. NO is a gasotransmitter produced by endothelial cells which readily diffuses across smooth muscle cells. NO responses include vascular smooth muscle relaxation, platelet aggregation inhibition, and neurotransmission, with implications in the respective organ systems' diseases. Vasodilation by NO is an important mechanism for homeostasis, maintaining appropriate blood pressure and blood flow.[21] The most sensitive physiologic receptor for nitric oxide is soluble guanylyl cyclase (sGC).[22]

sGC produces cyclic guanosine monophosphate (cGMP). NO binds to the heme prosthetic group of sGC, causing a conformation shift and activation of the enzyme. cGMP then acts as a secondary messenger, stimulating protein kinase G to phosphorylate further protein targets. cGMP is catabolized by phosphodiesterase (PDE) to 5'-GMP, at a rate 10-fold faster than cyclization of GMP. Thus, PDE is a target in cases where vasodilation is preferred, such as in hypertension or erectile dysfunction. Adequate amounts of NO are required for PDE targeting to be effective. Alternatively, the precursor of NO, L-arginine, can be given to patients as a supplement, promoting NO formation and lowering blood pressure.[23] A classic example of an NO-producing hypertension medication is nitroglycerin, Alfred Nobel's explosive that has a medical application as an antihypertensive agent. Patients can become tolerant to nitrates, reducing the long-term efficacy of these NO donors.

sGC itself is potentially a more suitable therapeutic target for cardiovascular disease. It is heterodimeric, composed of two subunits (α and β) which each have two isoforms. Only α_1/β_1 and α_2/β_1 heterodimers have been observed *in vivo*, with the former being more highly expressed. The enzyme is only active in the heterodimeric form under physiological conditions,[22] and requires a heme moiety for activity. The heme is coordinated by a His-105 residue on the β-subunit, and NO-coordination results in a hexa-coordinated histidine-heme-NO intermediate which rearranges to a penta-coordinated nitrosyl-heme complex. The loss of His-105 interaction causes the shift which activates the enzyme. However, recent X-ray spectroscopy suggests that complete dissociation of the histidine may not be required for activation.[24] Therapeutics which rely on the initial His-105 coordination to induce activation of sGC are termed heme-dependent, whereas heme-independent activators are more effective on the oxidized form of sGC.[25] Some heme-independent sGC activators include riociguat, ataciguat, and cinaciguat. Riociguat is approved for treatment of pulmonary arterial hypertension (PAH, WHO Group 1).[26] Mechanistically, it has a dual action on sGC by sensitizing the enzyme to endogenous NO as well as by acting as a direct stimulant.[27] Ataciguat and cinaciguat displace heme from the HNOX binding site and cause an effective conformational shift within the enzyme.[25]

Recently, gemfibrozil (Lopid, Figure 3.1), a fibrate used in the treatment of dyslipidemia, has been shown to be a heme-independent activator of sGC. It was determined to be unique within similar fibrates to be an sGC activator. Using truncated isoforms of sGC, the HNOX domain was shown to be important to gemfibrozil's activity. Gemfibrozil has been shown to have antiplatelet activity and causes vasodilation of aortic

rings but is less effective than cinaciguat and ataciguat. Molecular modelling of the HNOX binding domain with gemfibrozil suggests that two of the molecules may fit within the pocket, based on non-overlapping lowest-energy models (Figure 3.2).[28] Structurally, the molecule appears simple to make, and indeed has been synthesized through ether formation of the appropriate phenol with a protected ester and saponification to achieve gemfibrozil. An improved process paper using this strategy included results showing ~99.9% purity.[29]

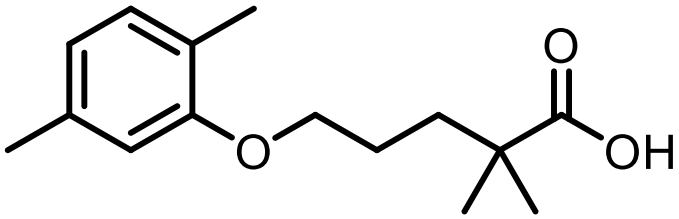

Figure 3.1. Structure of gemfibrozil.

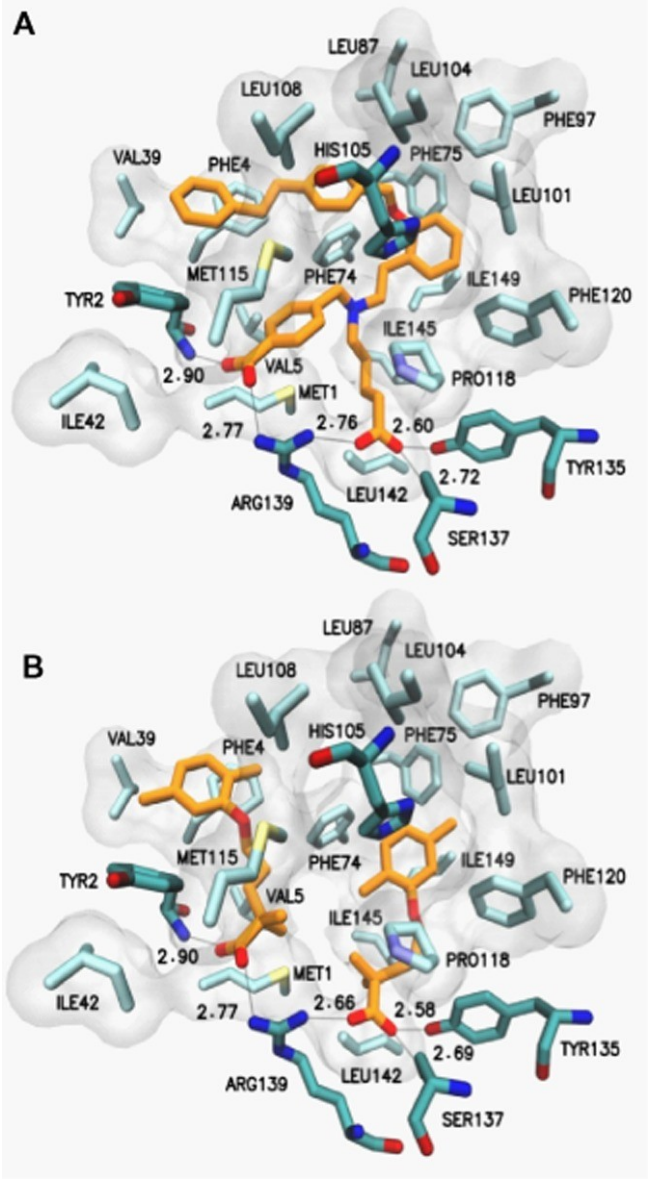

Figure 3.2. Molecular modeling of cinaciguat (A) and two molecules of gemfibrozil (B) to HNOX domain. (Reproduced from reference 28.)

The synthesis of gemfibrozil naturally lends itself to diversification by using a variety of phenols. This project was designed to help define a structure-activity relationship (SAR) of gemfibrozil analogs with varying aryl groups, evaluating steric and electronic effects of gemfibrozil derivatives on their ability to activate sGC. The

carboxylic acid moiety also provides a handle for analog syntheses via esterifications and peptide couplings. The goal of this work was to synthesize gemfibrozil analogs and screen them for sGC activity.

CHAPTER FOUR

Synthesis of Gemfibrozil Analogs

To the end of creating a series of analogs using different phenols, para-tert-butyl phenol was chosen as a first candidate. Starting with a chloride ester gemfibrozil precursor, an S_N2 reaction displacing the chloride by the phenol was performed. Saponification conditions were then chosen based on a process paper of gemfibrozil. This para-tert-butyl gemfibrozil analog is suspected to have been synthesized based on proton NMR, but it has not been further characterized. Attempts to reproduce this synthesis have thus far proven unsuccessful, possibly due to stopping the reaction early. Unfortunately, routine TLC monitoring of the first step tracking the ester disappearance is challenging, due to the low absorbance of the ester starting material and its difficulty being stained.

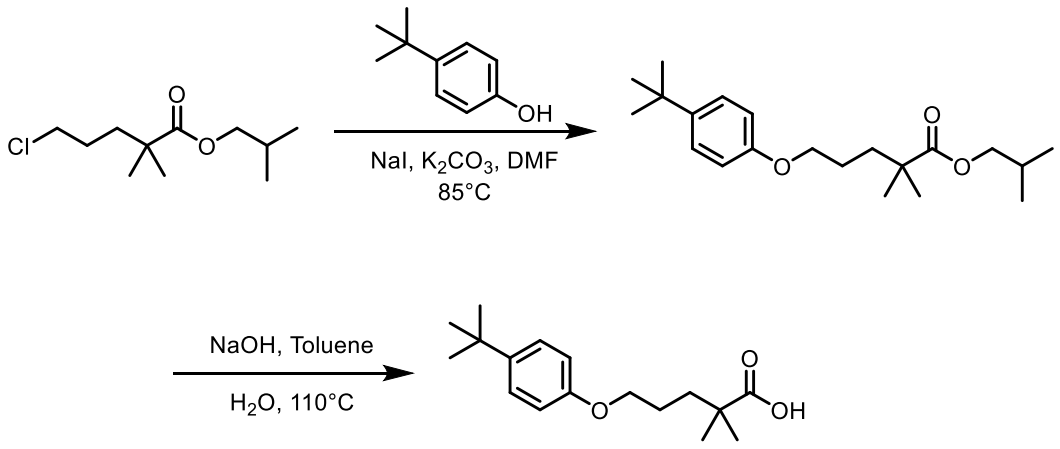

Scheme 4.1. Attempted synthesis of para-tert-butyl analog of gemfibrozil.

Amine coupling reactions to afford amide derivatives of gemfibrozil were attempted with n-butyl amine and hydrazine, using HATU as the coupling reagent. The n-butyl amide was synthesized once in 47% yield.

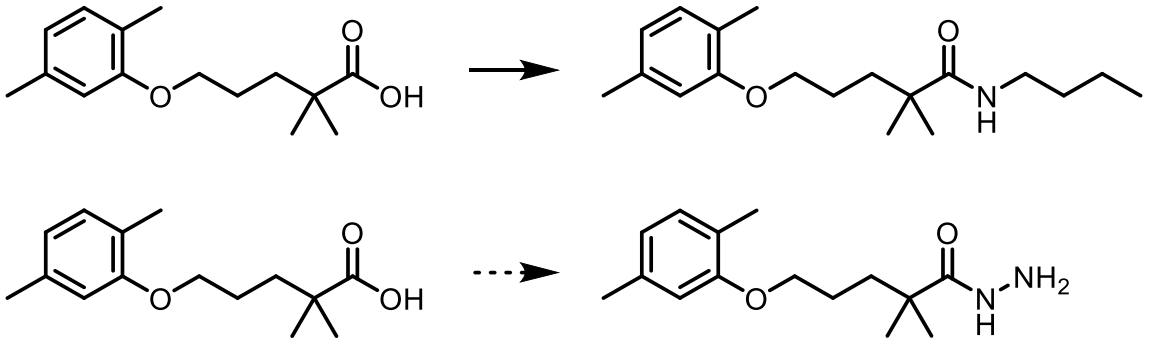

Scheme 4.2. Targets of couplings of gemfibrozil.

The synthesis of gemfibrozil analogs using various phenols as well as the preparation of amide derivatives by peptide coupling strategies remains promising, although this work is incomplete. Biological experiments on these and other gemfibrozil analogs synthesized in the Kane lab are currently being conducted by Dr. Martin's lab at the UT Health Science Center in Houston. These derivatives include dimers, which are of interest because of molecular modeling of an sGC HNOX domain, which showed that two gemfibrozil molecules could fit in one domain.[28]

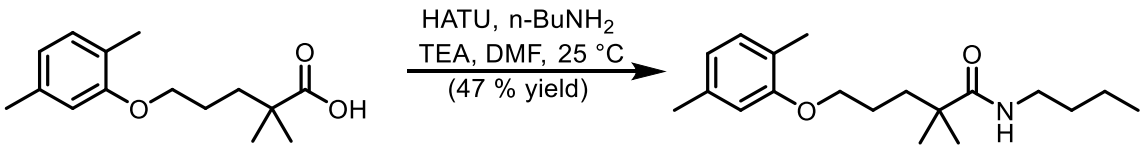

Scheme 4.3. Synthesis of Gemfibrozil n-Butyl Amide.

Gemfibrozil (50 mg, 0.2 mmol, 1 equiv.), HATU (76 mg, 0.2 mmol, 1 equiv.), TEA (27.9 µL, 0.2 mmol, 1 equiv.) and DMF (1 mL) were added to a 1-dram vial and stirred for 15 min at 25 °C. Then, n-butyl amine (98.6 µL, 1 mmol, 5 equiv.) was added and stirred for 23 h. Reaction was diluted with EtOAc, then washed with brine, 3 M HCl, then 1 M NaOH. Reaction mixture was purified with column chromatography using 40:60 EtOAc:Hex to provide 29 mg of a white solid in 47% yield.

^{1}**H NMR** (600 MHz, Chloroform-*d*) δ 7.00 (d, *J* = 7.5 Hz, 1H), 6.67 – 6.65 (d, *J* = 7.5 Hz 1H), 6.61 (s, 1H), 5.65 (t, *J* = 5.8 Hz, 1H), 3.92 (t, *J* = 6.0 Hz, 2H), 3.25 (td, *J* = 7.2, 5.6 Hz, 2H), 2.30 (s, 3H), 2.17 (s, 3H), 1.78 – 1.72 (m, 2H), 1.71 – 1.67 (m, 2H), 1.50 – 1.45 (m, 2H), 1.38 – 1.31 (m, 2H), 1.21 (s, 6H), 0.92 (t, *J* = 7.4 Hz, 2H).

^{13}C NMR (151 MHz, Chloroform-*d*) δ 177.3, 156.9, 136.5, 130.3, 123.5, 120.7, 112.1, 68.0, 41.8, 39.3, 37.6, 25.6, 25.1, 21.4, 20.1, 15.8, 13.8.

+ESI-HRMS m/z: calc'd for $[M+Na]^+$ $C_{19}H_{31}NNaO_2^+$ =328.2247, found $C_{19}H_{31}NNaO_2^+$ =328.2247.

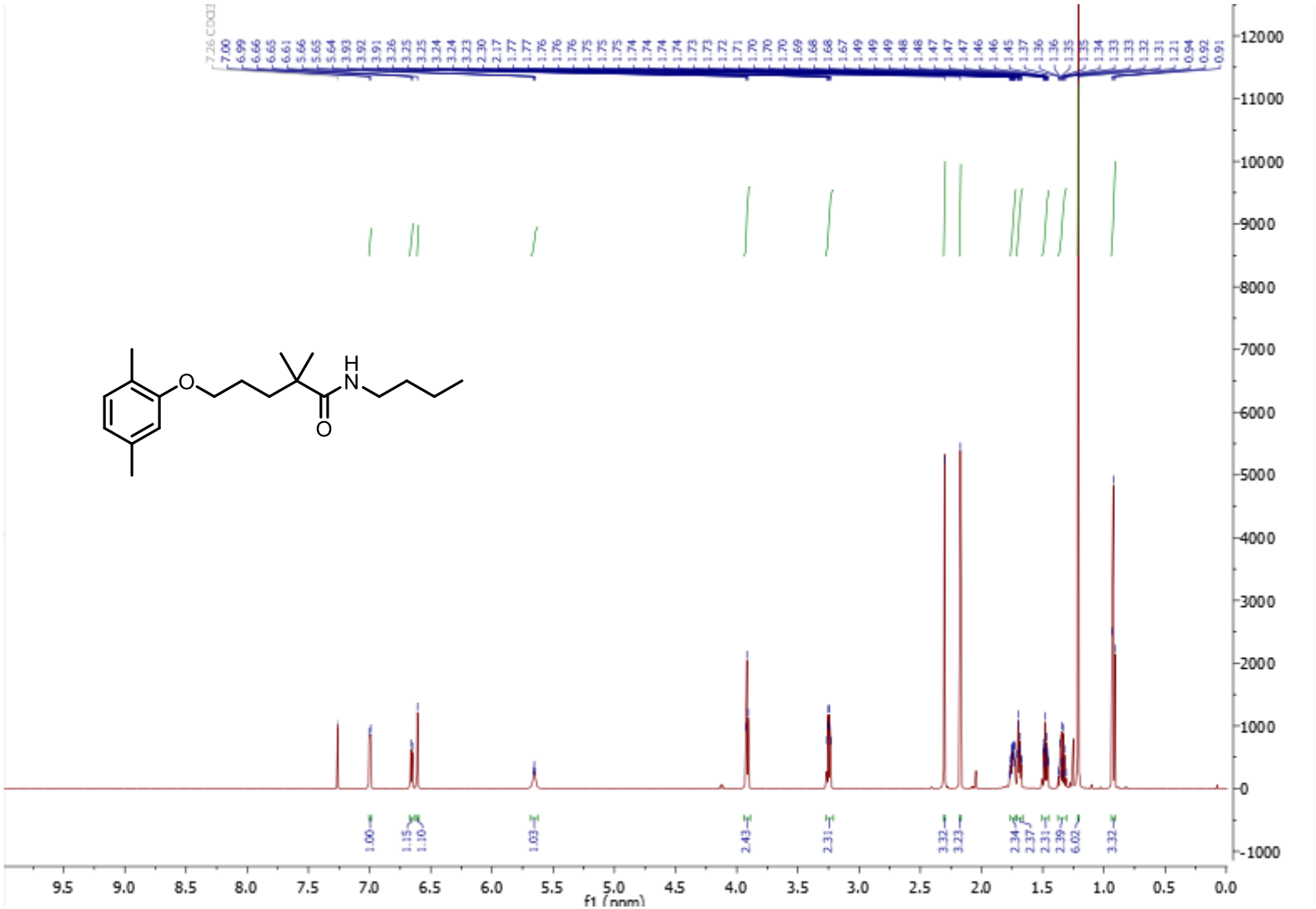

Figure 4.1. ^{1}H NMR of Gemfibrozil n-Butyl Amide.

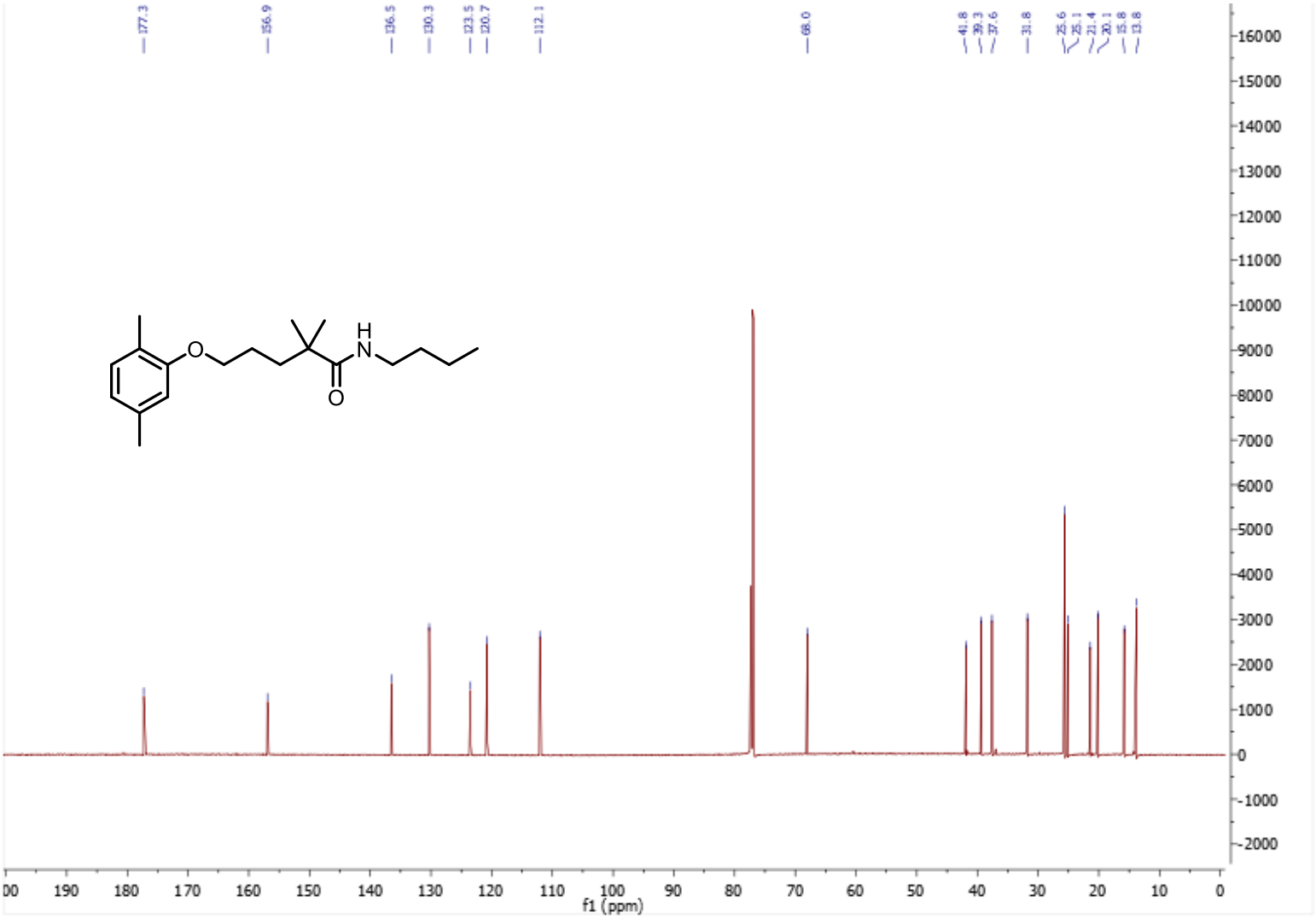

Figure 4.2. ^{13}C NMR of Gemfibrozil n-Butyl Amide.

REFERENCES

[1] Muzio, M.; Polentarutti, N.; Bosisio, D.; Manoj Kumar, P. P.; Mantovani, A. Toll-like Receptor Family and Signalling Pathway. *Biochem. Soc. Trans.* **2000**, *28* (5), 563–566. https://doi.org/10.1042/bst0280563.

[2] Dembic, Z. *The Function of Toll-Like Receptors*; Landes Bioscience, 2013.

[3] Lu, Y.-C.; Yeh, W.-C.; Ohashi, P. S. LPS/TLR4 Signal Transduction Pathway. *Cytokine* **2008**, *42* (2), 145–151. https://doi.org/10.1016/j.cyto.2008.01.006.

[4] Vaure, C.; Liu, Y. A Comparative Review of Toll-Like Receptor 4 Expression and Functionality in Different Animal Species. *Front. Immunol.* **2014**, *5*. https://doi.org/10.3389/fimmu.2014.00316.

[5] Alegre, M.-L.; Goldstein, D. R.; Chong, A. S. Toll-like Receptor Signaling in Transplantation. *Curr. Opin. Organ Transplant.* **2008**, *13* (4), 358–365. https://doi.org/10.1097/MOT.0b013e3283061149.

[6] Apetoh, L.; Ghiringhelli, F.; Tesniere, A.; Obeid, M.; Ortiz, C.; Criollo, A.; Mignot, G.; Maiuri, M. C.; Ullrich, E.; Saulnier, P.; Yang, H.; Amigorena, S.; Ryffel, B.; Barrat, F. J.; Saftig, P.; Levi, F.; Lidereau, R.; Nogues, C.; Mira, J.-P.; Chompret, A.; Joulin, V.; Clavel-Chapelon, F.; Bourhis, J.; André, F.; Delaloge, S.; Tursz, T.; Kroemer, G.; Zitvogel, L. Toll-like Receptor 4-Dependent Contribution of the Immune System to Anticancer Chemotherapy and Radiotherapy. *Nat. Med.* **2007**, *13* (9), 1050–1059. https://doi.org/10.1038/nm1622.

[7] Tsung, A.; Sahai, R.; Tanaka, H.; Nakao, A.; Fink, M. P.; Lotze, M. T.; Yang, H.; Li, J.; Tracey, K. J.; Geller, D. A.; Billiar, T. R. The Nuclear Factor HMGB1 Mediates Hepatic Injury after Murine Liver Ischemia-Reperfusion. *J. Exp. Med.* **2005**, *201* (7), 1135–1143. https://doi.org/10.1084/jem.20042614.

[8] Asea, A. Heat Shock Proteins and Toll-Like Receptors. In *Toll-Like Receptors (TLRs) and Innate Immunity*; Bauer, S., Hartmann, G., Eds.; Handbook of Experimental Pharmacology; Springer: Berlin, Heidelberg, 2008; pp 111–127. https://doi.org/10.1007/978-3-540-72167-3_6.

[9] Chang, C. A.; Akinbobuyi, B.; Quintana, J. M.; Yoshimatsu, G.; Naziruddin, B.; Kane, R. R. Ex-Vivo Generation of Drug-Eluting Islets Improves Transplant Outcomes by Inhibiting TLR4-Mediated NFkB Upregulation. *Biomaterials* **2018**, *159*, 13–24. https://doi.org/10.1016/j.biomaterials.2017.12.020.

[10] Chang, C. A.; Murphy, K.; Kane, R. R.; Lawrence, M. C.; Naziruddin, B. Early TLR4 Blockade Attenuates Sterile Inflammation-Mediated Stress in Islets During Isolation and Promotes Successful Transplant Outcomes. *Transplantation* **2018**, *102* (9), 1505. https://doi.org/10.1097/TP.0000000000002287.

[11] Rice, T. W.; Wheeler, A. P.; Bernard, G. R.; Vincent, J.-L.; Angus, D. C.; Aikawa, N.; Demeyer, I.; Sainati, S.; Amlot, N.; Cao, C.; Ii, M.; Matsuda, H.; Mouri, K.; Cohen, J. A Randomized, Double-Blind, Placebo-Controlled Trial of TAK-242 for the Treatment of Severe Sepsis. *Crit. Care Med.* **2010**, *38* (8), 1685–1694. https://doi.org/10.1097/CCM.0b013e3181e7c5c9.

[12] Matsunaga, N.; Tsuchimori, N.; Matsumoto, T.; Ii, M. TAK-242 (Resatorvid), a Small-Molecule Inhibitor of Toll-Like Receptor (TLR) 4 Signaling, Binds Selectively to TLR4 and Interferes with Interactions between TLR4 and Its Adaptor Molecules. *Mol. Pharmacol.* **2011**, *79* (1), 34–41. https://doi.org/10.1124/mol.110.068064.

[13] Takashima, K.; Matsunaga, N.; Yoshimatsu, M.; Hazeki, K.; Kaisho, T.; Uekata, M.; Hazeki, O.; Akira, S.; Iizawa, Y.; Ii, M. Analysis of Binding Site for the Novel Small-Molecule TLR4 Signal Transduction Inhibitor TAK-242 and Its Therapeutic Effect on Mouse Sepsis Model. *Br. J. Pharmacol.* **2009**, *157* (7), 1250–1262. https://doi.org/10.1111/j.1476-5381.2009.00297.x.

[14] Yamada, M.; Ichikawa, T.; Ii, M.; Sunamoto, M.; Itoh, K.; Tamura, N.; Kitazaki, T. Discovery of Novel and Potent Small-Molecule Inhibitors of NO and Cytokine Production as Antisepsis Agents: Synthesis and Biological Activity of Alkyl 6-(N-Substituted Sulfamoyl)Cyclohex-1-Ene-1-Carboxylate. *J. Med. Chem.* **2005**, *48* (23), 7457–7467. https://doi.org/10.1021/jm050623t.

[15] Hegarty, A. F.; Tynan, N. M.; Fergus, S. Rate-Determining Nitrogen Inversion in the Isomerisation of Isoimides to Imides and Azides to Tetrazoles: Direct Observation of Intermediates Stabilized by Trifluoroethyl Groups. *J. Chem. Soc. Perkin Trans. 2* **2002**, No. 7, 1328–1334. https://doi.org/10.1039/B202005J.

[16] Yamada, M.; Ichikawa, T.; Ii, M.; Sunamoto, M.; Itoh, K.; Tamura, N.; Kitazaki, T. Discovery of Novel and Potent Small-Molecule Inhibitors of NO and Cytokine Production as Antisepsis Agents: Synthesis and Biological Activity of Alkyl 6-(N-Substituted Sulfamoyl)Cyclohex-1-Ene-1-Carboxylate. *J. Med. Chem.* **2005**, *48* (23), 7457–7467. https://doi.org/10.1021/jm050623t.

[17] Kobayashi, T.; Saitoh, M.; Wada, Y.; Nara, H.; Negoro, N.; Yamasaki, M.; Tanaka, T.; Kitamoto, N. Cyclic Compound. US20180118708A1, May 3, 2018.

[18] Dijk, T. van; Slootweg, J. C.; Lammertsma, K. Nitrilium Ions – Synthesis and Applications. *Org. Biomol. Chem.* **2017**, *15* (48), 10134–10144. https://doi.org/10.1039/C7OB02533E.

[19] Trost, B. M.; Machacek, M. R.; Tsui, H. C. Development of Aliphatic Alcohols as Nucleophiles for Palladium-Catalyzed DYKAT Reactions: Total Synthesis of (+)-Hippospongic Acid A. *J. Am. Chem. Soc.* **2005**, *127* (19), 7014–7024. https://doi.org/10.1021/ja050340q.

[20] Baker, L.; Minehan, T. Efficient Palladium-Catalyzed Nucleophilic Addition of Triorganoindium Reagents to Carbocyclic Derivatives. *J. Org. Chem.* **2004**, *69* (11), 3957–3960. https://doi.org/10.1021/jo0357162.

[21] Horst, B. G.; Marletta, M. A. Physiological Activation and Deactivation of Soluble Guanylate Cyclase. *Nitric Oxide* **2018**, *77*, 65–74. https://doi.org/10.1016/j.niox.2018.04.011.

[22] Martin, E.; Berka, V.; Tsai, A.-L.; Murad, F. Soluble Guanylyl Cyclase: The Nitric Oxide Receptor. *Methods Enzymol.* **2005**, *396*, 478–492. https://doi.org/10.1016/S0076-6879(05)96040-0.

[23] Ahmad, A.; Dempsey, S. K.; Daneva, Z.; Azam, M.; Li, N.; Li, P.-L.; Ritter, J. K. Role of Nitric Oxide in the Cardiovascular and Renal Systems. *Int. J. Mol. Sci.* **2018**, *19* (9). https://doi.org/10.3390/ijms19092605.

[24] Dai, Z.; Farquhar, E. R.; Arora, D. P.; Boon, E. M. Is Histidine Dissociation a Critical Component of the NO/H-NOX Signaling Mechanism? Insights from X-Ray Absorption Spectroscopy. *Dalton Trans. Camb. Engl. 2003* **2012**, *41* (26), 7984–7993. https://doi.org/10.1039/c2dt30147d.

[25] Priviero, F. B. M.; Webb, R. C. Heme-Dependent and Independent Soluble Guanylate Cyclase Activators and Vasodilation. *J. Cardiovasc. Pharmacol.* **2010**, *56* (3), 229–233. https://doi.org/10.1097/FJC.0b013e3181eb4e75.

[26] Staff, P. H. A. Riociguat. *Pulmonary Hypertension Association*.

[27] Khaybullina, D.; Patel, A.; Zerilli, T. Riociguat (Adempas): A Novel Agent For the Treatment of Pulmonary Arterial Hypertension and Chronic Thromboembolic Pulmonary Hypertension. *Pharm. Ther.* **2014**, *39* (11), 749–758.

[28] Sharina, I. G.; Sobolevsky, M.; Papakyriakou, A.; Rukoyatkina, N.; Spyroulias, G. A.; Gambaryan, S.; Martin, E. The Fibrate Gemfibrozil Is a NO- and Haem-Independent Activator of Soluble Guanylyl Cyclase: In Vitro Studies. *Br. J. Pharmacol.* **2015**, *172* (9), 2316–2329. https://doi.org/10.1111/bph.13055.

[29] Madasu, S. B.; Vekariya, N. A.; Velladurai, H.; Islam, A.; Sanasi, P. D.; Korupolu, R. B. Improved Process for Preparation of Gemfibrozil, an Antihypolipidemic. *Org. Process Res. Dev.* **2013**, *17* (7), 963–966. https://doi.org/10.1021/op400034f.